

Quantum critical benchmark for density functional theory

Paul E. Grabowski^{1,*} and Kieron Burke^{2,†}

¹*Department of Chemistry, University of California, Irvine, CA 92697, USA*

²*Departments of Chemistry and Physics, University of California, Irvine, CA 92697, USA*

Two electrons at the threshold of ionization represent a severe test case for electronic structure theory. A pseudospectral method yields a very accurate density of the two-electron ion with nuclear charge close to the critical value. Highly accurate energy components and potentials of Kohn-Sham density functional theory are given, as well as a useful parametrization of the critical density. The challenges for density functional approximations and the strength of correlation are also discussed.

The value of highly accurate benchmark calculations to first-principles electronic structure theory cannot be overstated. While comparison with experiment is the ultimate arbiter of the usefulness of prediction, the ability to control and eliminate multiple sources of error with a direct solution of the Schrödinger equation allows pure ‘apples-to-apples’ comparisons. These have proven invaluable in the development of Kohn-Sham (KS) density functional theory (DFT) [1], where the methodology is so alien to standard wave function treatments that usually only a detailed comparison of ground-state energies can be used to test approximations. For a recent example, van der Waals theories use highly accurate quantum chemical methods on small molecules to validate (or not) approximate functionals, not just at equilibrium bond lengths, but for entire binding energy curves [2]. Accurate energies and densities can also be used to distinguish energy-driven from density-driven errors in DFT [3].

Beyond ground-state energy comparisons, various energy components and potentials can be examined, once a sufficiently accurate density is available from the benchmark calculation. The pioneering work of Umrigar and coworkers [4, 5] for several spherical atoms is a case in point. The availability of the KS potential and its eigenvalues was useful for all DFT, and especially for the development of linear-response time-dependent density functional methods for finding excited state energies, where the ground-state orbitals and energies are vital inputs [6]. A similar role was played by Baerends and coworkers for the H_2 molecule as a function of bond length [7]. This system has since become the paradigm of strong correlation [8].

The benchmark we consider here is, in some ways, the most fundamental to electronic structure theory: two electrons bound to a single nucleus. But we study the very special case when the ionization potential is precisely zero, i.e., the nuclear charge Z_c is the smallest possible value that binds two electrons. Thus the density is the most diffuse of any single-center electronic system, making it extremely difficult to extract from most methods. For example, traditional quantum chemical basis sets fall off too rapidly at large r to extract the den-

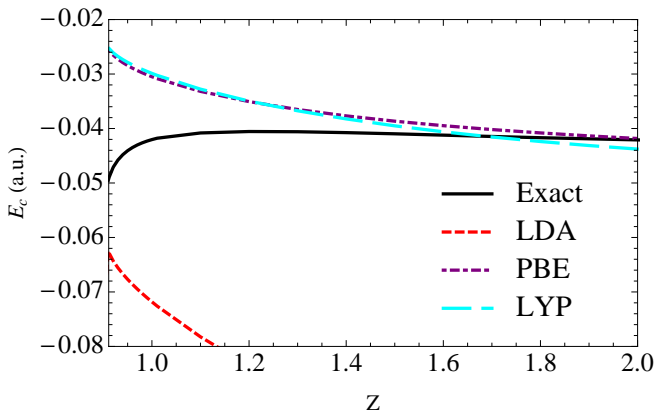


FIG. 1. Exact and approximate correlation energies, evaluated with the exact densities.

sity, even if the energy is extremely accurate. This is the simplest case of a quantum-critical electronic problem [9]. Such systems have been mapped to phase transitions in statistical mechanics [10].

Recently, high-precision variational calculations have greatly expanded the accuracy to which Z_c is known [11], and esoteric strong correlation methods have been tested on this system [12]. Our work shows how pseudospectral methods are ideally suited for extracting expectation values for weakly bound systems, demonstrated by an extremely accurate density at Z_c . We parametrize this density in a simple form, give the asymptotic density at large r to order r^{-4} and highly accurate KS energy components, and show the performance of popular DFT approximations.

The usefulness of our benchmark is illustrated in Fig. 1. Previous calculations [4] for two-electron ions run from $Z = 80$ (Hg^{78+}) down to $Z = 1$ (H^-). The correlation energy is almost independent of Z , and is roughly accounted for by modern approximations down to $Z = 2$ (He). But the slope of $E_c(Z)$ changes sign below 2, an effect completely missed by the commonly used functionals, PBE [13] and LYP [14, 15], which behave more poorly as the density becomes more diffuse. (But see the end of this letter, where this apparent catastrophe for modern approximations mysteriously becomes a triumph!).

For many N -electron atoms, there exists a minimum $Z_c = N - 1 - \nu$, with $0 < \nu < 1$, such that the ground

* paul.grabowski@uci.edu

† kieron@uci.edu

state of $\hat{H}(Z)$ has positive ionization energy for all nuclear charges $Z > Z_c$. It is thought that $\lambda_c = 1/Z_c$ corresponds to the radius of convergence of the perturbative solution of the two-electron atom with the perturbation being the electron-electron interaction $1/r_{12}$ [16]. Baker and coworkers used 401 orders of perturbation theory to obtain $Z_c = 0.911\,03$ [16] and Ivanov later used better extrapolation techniques on their data to get $Z_c = 0.911\,028\,26$ [17]. From a direct variational calculation to solve for the critical charge, Sergeev and Kais obtained $Z_c = 0.911\,028\,225$ [18]. Recently, Estienne and coworkers [11] obtained $Z_c = 0.911\,028\,224\,077\,255\,73(4)$, far surpassing the prior estimates in precision. In the present work, we obtain $Z_c = 0.911\,028\,224\,07(6)$, agreeing with Ref. [11] and an unpublished figure by Schwartz [19]. Although our critical charge is not as precise, our wave function is roughly as accurate as our value of Z_c , allowing the calculation of much more precise expectation values than a variational calculation [20].

Standard quantum methods typically have much trouble calculating states near the ionization threshold. Such difficulties stem from two reasons: an improper representation of the wave function near the electron-electron coalescence point and the mixing of energetically similar continuum states into the ground state when using an approximate method. For example, diffusion Monte Carlo calculations take advantage of the separation in energy between the ground state and excited states and fails to separate degenerate states. However, the pseudospectral method is a non-variational collocation method in which the value of the wave function is calculated on a grid in such a way that the *local* error in the wave function becomes exponentially small with increasing grid resolution. It allows us to accurately calculate the bound state right on the threshold of the continuum by automatically selecting normalizable states.

Pseudospectral methods [21] have their origins in fluid dynamics [22], for which they are used to evolve systems without shocks because their convergence properties only hold for \mathcal{C}^∞ functions. They have been extended to solving Einstein's field equations for colliding black holes by the excision of the singularities from the computational domain [23, 24]. In quantum chemistry, Friesner and others have shown orders of magnitude improvement in speed for a wide variety of methods [25–33]. Direct solution of Schrödinger's equation has been done for one-electron problems [34, 35], but only recently has a sufficient representation of the computational domain been demonstrated for the case of fully-correlated, multi-electron atoms [20, 36]. Here we use the same implementation as in Ref. [20].

To illustrate the strength of the local convergence property, we plot in Fig. 2, $\kappa = (1/2)d\log(n)/dr$, where $n(r)$ is the one-electron density, for $Z = Z_c$ and $Z = 1$ (H^-). As $r \rightarrow \infty$, for $Z > Z_c$, the well-known analysis of the exponential decay of the density [37] yields $\kappa \rightarrow -\sqrt{2I}$, where I is the ionization energy. However, for $Z = Z_c$, the behavior differs qualitatively

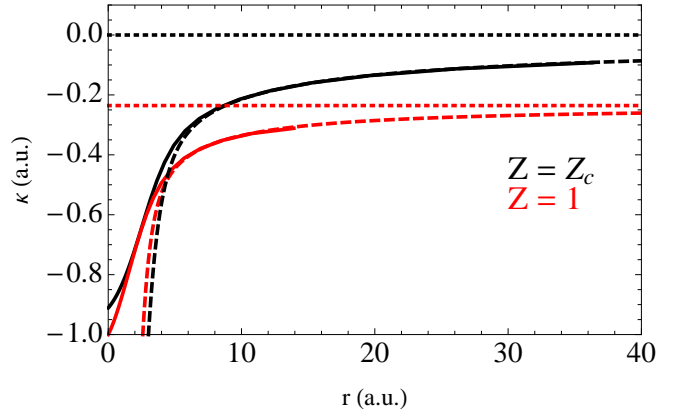


FIG. 2. Logarithmic derivative of the density ($2\kappa = d\ln n/dr$) as a function of r for $Z = Z_c$ (upper, black) and $Z = 1$ (lower, red). Solid lines are calculated. The limits at large r are shown as dotted lines and results of using Eqs. (4) and (5) are shown as the dashed lines.

($\kappa \rightarrow -2\sqrt{2(1-Z_c)/r}$). For both values of Z , the asymptotic value is not approached until very large r . Even at $r = 40$ Bohr, there is a visible deviation in $\kappa(r)$ from its limits, so one must use higher order expansions to connect the limits with our numeric results.

To analyze these results, we review well-known facts from KS DFT [38]. The KS equations describe fictitious non-interacting fermions sitting in a potential, $v_s(\mathbf{r})$, whose density matches the real one. For two spin-unpolarized electrons, one orbital is doubly occupied and the KS equation in atomic units is

$$\left[-\frac{1}{2}\nabla^2 + v_s(\mathbf{r})\right]\phi(\mathbf{r}) = \epsilon\phi(\mathbf{r}), \quad (1)$$

where $\phi = \sqrt{n(r)/2}$ and $\epsilon = -I = E + Z^2/2$ are the KS orbital and its energy, respectively, while $v_s(r)$ is the Kohn-Sham potential given by

$$v_s(\mathbf{r}) = -\frac{Z}{r} + v_H(\mathbf{r}) + v_X(\mathbf{r}) + v_C(\mathbf{r}). \quad (2)$$

For two electrons, the Hartree and exchange potentials are trivially related,

$$v_H(\mathbf{r}) = -2v_X(\mathbf{r}) = \int \frac{n(\mathbf{r}')d\mathbf{r}'}{|\mathbf{r} - \mathbf{r}'|} \quad (3)$$

and the correlation potential is defined so as to make Eq. (1) exact. For large r , the exchange potential, behaves as $-1/r$ while the correlation potential decays much faster, as $-\alpha/2r^4$, where α is the dipole polarizability of the $N - 1$ system, here equal to $9/2Z^4$ [4]. Amovilli and March [39] derived the asymptotic behavior of the density at large r for $Z = 2$. Here, we extend their work to any $Z > Z_c$ and to the next highest order in $1/r$:

$$\sqrt{n_Z(r)} \sim \frac{x^\beta \sqrt{A}}{e^x} \left[\sum_{k=0}^4 \frac{a_k}{x^k} - \frac{3r^{-2}}{4Z^4} \sum_{k=1}^2 \frac{\tilde{a}_k}{x^k} + \mathcal{O}(x^{-5}) \right], \quad (4)$$

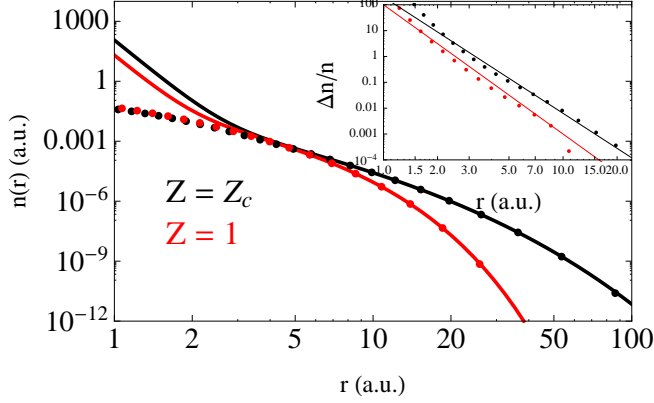


FIG. 3. Exact (dots) and asymptotic ($A = 0.005528$ and $B = 0.1375$) densities (solid line) for $Z = Z_c$ (upper, black) and $Z = 1$ (lower, red). The fractional error (dots) in the asymptotic forms is shown in the inset along with curves proportional to $r^{-4.5}$ (upper, black) and r^{-5} (lower, red).

where $\delta = Z - Z_c$, $x = \eta r$, $\eta = \sqrt{2I}$, $\beta = \xi/\eta - 1$, and $\xi = Z - 1$. The constant A is defined as $A = \lim_{r \rightarrow \infty} n_Z(r) e^{2x}/x^{2\beta}$. The formula $A = \alpha_1 \delta + \alpha_2 \delta^2 + \alpha_3 \delta^3$, with $\alpha_1 = 0.00667448$, $\alpha_2 = 0.567102$, and $\alpha_3 = 2/\pi$ fits our densities over the entire Z range to within 0.2% with the maximum error occurring around $Z = 1$.

The value of α_3 comes from the large- Z limit of the density. Likewise, $I = \{1 + \beta_1 \exp[-\beta_2 \ln^2(\beta_3 \delta)]\}(\beta_4 \delta + \delta^2/2)$, with $\beta_1 = 0.0857048$, $\beta_2 = 0.166941$, $\beta_3 = 5.097253$, and $\beta_4 = 2\langle 1/r_1 \rangle_{Z=Z_c} - Z_c = 0.24518901$ has a maximum error of 0.3% occurring around $Z = 0.92$. The coefficients in the large- r expansion are given recursively as $a_0 = 1$, $a_k = -a_{k-1}[\xi - k\eta][\xi - (k-1)\eta]/(2k\eta^2)$, and $\tilde{a}_0 = 1$ and $\tilde{a}_1 = -(\beta^2 + \beta + 3)/2$.

At Z_c , the long range behavior changes [12, 39, 40]. Here we extend such asymptotic forms to higher order:

$$\sqrt{n_{Z_c}(r)} \sim \frac{\sqrt{B}e^{-y}}{r^{3/4}} \left[\sum_{k=0}^8 \frac{b_k}{y^k} - \frac{9r^{-2}}{4Z_c^4} \sum_{k=1}^4 \frac{\tilde{b}_k}{y^k} + \mathcal{O}(y^{-9}) \right], \quad (5)$$

where $B = \lim_{r \rightarrow \infty} n_{Z_c}(r) e^{2y} y^{3/2} \approx 0.1375$, $y = 2\sqrt{2}|\xi_c|r$, $\xi_c = Z_c - 1$, and $b_0 = 1$, $b_k = -b_{k-1}(2k+1)(2k-3)/8k$, while $\tilde{b}_1 = 4/5$, $\tilde{b}_2 = -17/10$, $\tilde{b}_3 = 1107/224$, and $\tilde{b}_4 = -30489/1792$. We have shown these asymptotic limits along with our calculated densities in Fig. 3 for both $Z = Z_c$ and 1. The error in the asymptotic forms decreases with increasing r at the expected rates.

To make our results more immediately useful for testing density functionals, we created a fit to the critical density:

$$n_{Z_c}(r) = \left[n_0 e^{-2Z_c r} \left(1 + \sum_{k=1}^8 \frac{c_k}{2^{k^2/4}} r^{k+1} \right) + B \frac{r^3}{s^3 + r^3} \left(\frac{a}{\tilde{y}} \right)^3 \frac{e^{-\tilde{y}}}{1 - \frac{3}{2\tilde{y}} + \frac{21}{8\tilde{y}^2} - \frac{87}{16\tilde{y}^3} + \frac{1755}{128\tilde{y}^4}} \right] \left[1 + \frac{d_1 r^{10}}{1 + d_2 r^{29/2}} \right] \quad (6)$$

n_0	0.23819008067	B	0.1375
c_1	0.0610986	c_2	0.0352145
c_3	-0.0494222	c_4	0.123575
c_5	-0.212456	c_6	0.308266
c_7	-0.328053	c_8	0.219550
d_1	7.82582×10^{-5}	d_2	3.79484
s	4.19599		

TABLE I. Parameters for Eq. (6).

where $\tilde{y} = (2y)^4/\sqrt{1+(2y)^6}$, $a = 4\sqrt{2}|\xi_c|$, $n_0 = 2\langle \delta(r_1) \rangle$, and the fit parameters (c_k 's and d_k 's) are given in Tab. I. The short-range part is exact to first order in r and along with the long-range part contains higher order corrections to order r^9 by fitting to the pseudospectral density. The long-range part is chosen to reproduce Eq. (5) to order r^{-2} , while the last term is a Padé approximate to the remaining error. For a more accurate density, we provide our raw data in the supplemental information.

For two unpolarized electrons, the ground-state energy and all KS energy components can be extracted directly

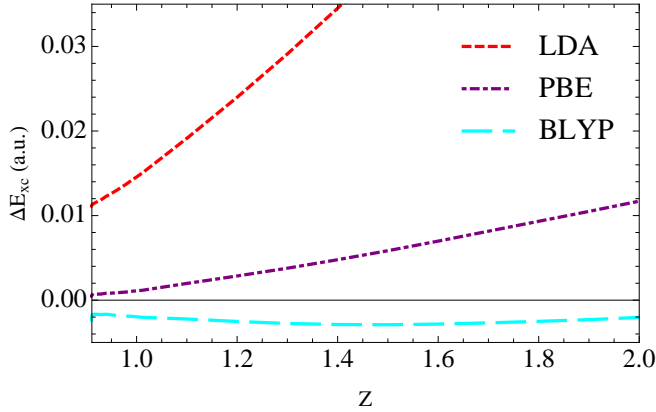
	Pseudospectral	fit
N	1.9999118	1.99757
E	-0.41498621252(5)	
E_H	0.595467(52)	0.595038
T_S	0.389857(17)	0.389873
E_n	-1.053346537(20)	-1.053176
E_C	-0.049240(39)	-0.049202
T_C	0.025129(17)	0.0251133

TABLE II. Normalization and energy components (total, Hartree, Kohn-Sham kinetic, nuclear, correlation, and kinetic correlation) of the critically bound system.

from the density and external potential without solving an interacting problem [4]. We perform this procedure here as a test of the accuracy of our densities. These energies are listed in Table II for $Z = Z_c$ for both our pseudospectral density and our parametrized form [Eq. (6)]. The errors in this form are $\sim 0.1\%$ or less. Thus this fit can be used to test approximate functionals on, if this level of accuracy is sufficient. In the supplemental info, we give tables of more accurate densities.

	$Z = Z_c$	$Z = 2$ Ref. [20]
$\langle r_1^2 \rangle$	39.779 95(20)	1.193 482 995 30(16)
$\langle r_{12}^2 \rangle$	81.303 37(40)	2.516 439 313 8(6)
$\langle \mathbf{r}_1 \cdot \mathbf{r}_2 \rangle$	-0.871 728 2(66)	-0.064 736 661 60(25)
$\langle r_1 \rangle$	4.146 972 44(58)	0.929 472 295 02(6)
$\langle r_{12} \rangle$	7.083 427 6(12)	1.422 070 255 93(38)
$\langle 1/r_1 \rangle$	0.578 108 619(11)	1.688 316 800 5(6)
$\langle 1/r_{12} \rangle$	0.223 374 112(19)	0.945 818 448 5(6)
$\langle 1/r_1^2 \rangle$	0.873 035 760 4(46)	6.017 408 866 1(36)
$\langle 1/r_{12}^2 \rangle$	0.085 788 151 9(80)	1.464 770 922 4(15)
$\langle 1/r_1 r_2 \rangle$	0.239 016 167(21)	2.708 655 473 6(20)
$\langle 1/r_1 r_{12} \rangle$	0.154 038 646(14)	1.920 943 921 1(13)
$\langle \delta(r_1) \rangle$	0.157 506 390 55(31)	1.810 429 318 2(12)
$\langle \delta(r_{12}) \rangle$	0.001 473 985 59(13)	0.106 345 370 53(33)

TABLE III. Expectation values in atomic units.

FIG. 4. Error in approximate exchange-correlation energies, evaluated with the exact densities. The error in the PBE energy at $Z = Z_c$ is 6×10^{-4} hartree.

We also give expectation values of some simple operators in Tab. III, compared to those for the helium atom. We can see that at the critical value, the two-electron atom is much fatter than for $Z = 2$. Furthermore, we can determine that it is much more likely that the two electrons are on opposite sides of the nucleus than for $Z = 2$ from the expectation value of $\mathbf{r}_1 \cdot \mathbf{r}_2$, which has a value more than an order of magnitude greater.

To conclude, we discuss whether this system ought to be considered *strongly correlated*, as in Ref. [12]. By sev-

eral naive criteria, we would say that it is. The fact that standard density functional approximations fail so badly for the correlation energy is one. In fact, if performed self-consistently, such calculations lose a fraction of an electron to the aether [3]. Another is the fact that, in a Hartree-Fock calculation, this system would be unbound because its HF energy is above that of the single ion. Finally, the ratio of correlation to exchange energy, and of kinetic correlation to correlation energy are both smallest for $Z = Z_c$. For weakly correlated systems, that ratio is almost 1, whereas here it is close to $1/2$.

On the other hand, DFT requires approximating both exchange and correlation together, and is notorious for cancellations of errors between these two. For Z_c , not only are the exchange and correlation potentials qualitatively incorrect in ways similar to Ref. [4], but also the exchange and correlation energies are each off by about a factor of two. However, these energy errors almost exactly cancel. The error in the exchange-correlation energy using the PBE functional on the exact density is less than a milliHartree (see Fig. 4)! All functionals become more accurate as $Z \rightarrow Z_c$, demonstrating the mysterious power of these approximations. By this criterion, these are not strongly correlated systems, which explains why the SCE approach of Ref. [12] does not yield better energetics here.

In summary, we have calculated highly precise wave functions at and near the critical value of Z which has zero ionization energy for a two-electron atom. We have shown that the correlation energy as a function of Z behaves in a qualitatively different manner than standard DFT approximations near $Z = Z_c$. Asymptotic expressions for the densities at large r to order r^{-4} were derived for all values $Z \geq Z_c$ and fits were given for the coefficient and ionization energies needed for these expressions. We gave an accurate fit for the critical density and showed that it reproduces all DFT energies and many expectation values of our exact numerical expression to about 0.1% or less. This fit can easily be used by others to check their DFT approximations. Of further use, are the many expectation values we calculate directly from our wave function. Lastly, we conclude that this critically bound system is not strongly correlated because its energy is well represented by commonly used GGA's.

We gratefully acknowledge funding from the National Science Foundation (grant number CHE-1112442).

-
- [1] W. Kohn and L. J. Sham, *Phys. Rev.* **140**, A1133 (1965).
 - [2] J. Klimeš and A. Michaelides, *The Journal of Chemical Physics* **137**, 120901 (2012).
 - [3] M.-C. Kim, E. Sim, and K. Burke, *Phys. Rev. Lett.* **111**, 073003 (2013).
 - [4] C. J. Umrigar and X. Gonze, *Phys. Rev. A* **50**, 3827 (1994).
 - [5] C.-J. Huang and C. J. Umrigar, *Phys. Rev. A* **56**, 290 (1997).
 - [6] H. Appel, E. K. U. Gross, and K. Burke, *Phys. Rev. Lett.* **90**, 043005 (2003).
 - [7] M. A. Buijse, E. J. Baerends, and J. G. Snijders, *Phys. Rev. A* **40**, 4190 (1989).
 - [8] P. Mori-Sánchez, A. J. Cohen, and W. Yang, *Phys. Rev. Lett.* **100**, 146401 (2008).
 - [9] P. Serra and S. Kais, *Phys. Rev. Lett.* **77**, 466 (1996).
 - [10] J. P. Neirotti, P. Serra, and S. Kais, *Phys. Rev. Lett.* **79**, 3142 (1997).

-
- [11] C. S. Estienne, M. Busuttil, A. Moini, and G. W. F. Drake, *Phys. Rev. Lett.* **112**, 173001 (2014).
 - [12] A. Mirtschink, C. J. Umrigar, J. D. Morgan, and P. Gori-Giorgi, *The Journal of Chemical Physics* **140**, 18A532 (2014).
 - [13] J. P. Perdew, K. Burke, and M. Ernzerhof, *Phys. Rev. Lett.* **77**, 3865 (1996), *ibid.* **78**, 1396(E) (1997).
 - [14] C. Lee, W. Yang, and R. G. Parr, *Phys. Rev. B* **37**, 785 (1988).
 - [15] B. Miehlisch, A. Savin, H. Stoll, and H. Preuss, *Chem. Phys. Lett.* **157**, 200 (1989).
 - [16] J. D. Baker, D. E. Freund, R. N. Hill, and J. D. Morgan, *Phys. Rev. A* **41**, 1247 (1990).
 - [17] I. A. Ivanov, *Phys. Rev. A* **51**, 1080 (1995).
 - [18] A. V. Sergeev and S. Kais, *Journal of Physics A: Mathematical and General* **32**, 6891 (1999).
 - [19] C. Schwartz, “Perturbation theory and threshold bound state for two electron atom,” unpublished (2013).
 - [20] P. E. Grabowski and D. F. Chernoff, *Phys. Rev. A* **84**, 042505 (2011).
 - [21] W. H. Press, S. A. Teukolsky, W. T. Vetterling, and B. P. Flannery, *Numerical Recipes: The Art of Scientific Computing*, third edition ed. (Cambridge University Press, 32 Avenue of the Americas, New York, NY 10013-2473, USA, 2007).
 - [22] C. Canuto, M. Hussaini, A. Quarteroni, and T. Zang, *Spectral Methods in Fluid Dynamics* (Springer, Berlin, 1988).
 - [23] L. E. Kidder and L. S. Finn, *Phys. Rev. D* **62**, 084026 (2000).
 - [24] H. P. Pfeiffer, L. E. Kidder, M. A. Scheel, and S. A. Teukolsky, *Comput. Phys. Commun.* **152**, 253 (2003).
 - [25] R. A. Friesner, *Chem. Phys. Lett.* **116**, 39 (1985).
 - [26] R. A. Friesner, *J. Chem. Phys.* **85**, 1462 (1986).
 - [27] R. A. Friesner, *J. Chem. Phys.* **86**, 3522 (1987).
 - [28] M. N. Ringnalda, M. Belhadj, and R. A. Friesner, *J. Chem. Phys.* **93**, 3397 (1990).
 - [29] B. H. Greeley, T. V. Russo, D. T. Mainz, R. A. Friesner, J.-M. Langlois, W. A. Goddard, III, J. Robert E. Donnelly, and M. N. Ringnalda, *J. Chem. Phys.* **101**, 4028 (1994).
 - [30] R. B. Murphy, M. D. Beachy, R. A. Friesner, and M. N. Ringnalda, *J. Chem. Phys.* **103**, 1481 (1995).
 - [31] R. B. Murphy, Y. Cao, M. D. Beachy, M. N. Ringnalda, and R. A. Friesner, *J. Chem. Phys.* **112**, 10131 (2000).
 - [32] C. Ko, D. K. Malick, D. A. Braden, R. A. Friesner, and T. J. Martínez, *J. Chem. Phys.* **128**, 104103 (2008).
 - [33] J. S. Heyl and A. Thirumalai, *Mon. Not. R. Astron. Soc.* (2010).
 - [34] A. G. Borisov, *J. Chem. Phys.* **114**, 7770 (2001).
 - [35] J. P. Boyd, C. Rangan, and P. H. Bucksbaum, *J. Comput. Phys.* **188**, 56 (2003).
 - [36] P. E. Grabowski and D. F. Chernoff, *Phys. Rev. A* **81**, 032508 (2010).
 - [37] J. P. Perdew, R. G. Parr, M. Levy, and J. L. Balduz, *Phys. Rev. Lett.* **49**, 1691 (1982).
 - [38] R. M. Dreizler and E. K. U. Gross, *Density Functional Theory: An Approach to the Quantum Many-Body Problem* (Springer-Verlag, Berlin, 1990).
 - [39] C. Amovilli and N. H. March, *Journal of Physics A: Mathematical and General* **39**, 7349 (2006).
 - [40] M. Hoffmann-Ostenhof, T. Hoffmann-Ostenhof, and B. Simon, *Journal of Physics A: Mathematical and General* **16**, 1125 (1983).
-

I. SUPPLEMENTAL INFORMATION

In the main body of the paper, we gave a fit to our density at $Z = Z_c$. This fit gave DFT energies to 0.1% or less. For those readers requiring more accuracy, we provide our best calculation of the one-electron density in Tab. IV. The accuracy of these data can be inferred from the value of our normalization in Tab. II, which is off by 9×10^{-5} . The majority of this error comes from the relatively large errors in the tail of the density. Since the weight for the density at the furthest out nonzero value is about 3×10^6 , the error in the density values is about 3×10^{-11} , comparable to the error in our value of Z_c .

In order to obtain a functional form that can be easily evaluated off the grid or used to calculate derivatives, one should construct the Cardinal functions:

$$C_j(x) = \prod_{k=1, k \neq j}^N \frac{x - x_k}{x_j - x_k}, \quad (7)$$

where $x = (1 - Z_c r)/(1 + Z_c r)$ and $N = 52$, which have the property of being equal to one at one grid point and zero at all the others. The density at an arbitrary value of x can then be obtained by

$$n(x) = \sum_{k=1}^N n_j C_j(x), \quad (8)$$

the explicit values used for n_j are in Tab. IV (note, values in the table are divided by Z_c^3).

Integration can be performed via quadrature. The values of x_j are the Gaussian quadrature points (roots of the 53rd order Legendre polynomial). For example,

$$\int dr n(r) = \frac{1}{Z_c^3} \sum_{j=1}^N w_j n_j, \quad (9)$$

where the values of w_j can be found in Tab. IV. Note, that the volume element $4\pi r^2 dr$ and the conversion from the r -coordinate to x -coordinate have already been taken into account by the values of w_j . Since the weights get rather large when r_j is big and the precision of the density is not very good in the tail, one should be careful about including such points in the quadrature. Usually some sort of truncation scheme is needed, chosen at a value of r such that contributions from larger r should be negligible.

r_j (a.u.)	x_j (a.u.)	n_j/Z_c^3 (a.u.)	w_j (a.u.)
0.0005759641912909017	0.9989511111039503	0.314682351915279	4.660741235847267e-9
0.00303925808565137	0.9944775909292161	0.3132732840892592	3.0300099503007153e-7
0.007489495670215863	0.9864461956515499	0.3107441016739011	2.9066843483625716e-6
0.013959796221790716	0.9748838842217445	0.30710436909115857	0.000013877890940302966
0.02249735397316229	0.9598318269330866	0.3023689171597749	0.00004612340448161165
0.03316494107684804	0.9413438536413591	0.29655769404226007	0.00012288064229107963
0.046041970051123156	0.9194861289164246	0.28969610387322686	0.00028224923029420383
0.061225781649952314	0.8943368905344953	0.2818154628129142	0.0005832308520293945
0.07883324279239258	0.8659861628460676	0.27295353887455004	0.0011139006628788277
0.09900270777331016	0.8345354323267345	0.2631551627930131	0.0020025658396714803
0.12189640224230178	0.8000972834304684	0.252472896572073	0.0034331010464428006
0.147703303023036	0.7627949951937449	0.24096774168832766	0.005666131691016764
0.17664260478943944	0.7227620997499832	0.22870986212496724	0.009068430900444735
0.2089678872961224	0.6801419042271677	0.21577928855460538	0.014153905827555817
0.24497212550105105	0.6350869776952459	0.20226655892230294	0.021641025428937748
0.28499372130027406	0.5877586049795791	0.18827323726105366	0.032533717316659924
0.32942378214164697	0.5383262092858274	0.17391223683317283	0.04823599283798371
0.3787149317776135	0.48696674569809606	0.15930785598077488	0.07071540224691103
0.43339201631982543	0.4338640677187617	0.14459541626218037	0.10273774745849322
0.4940651706915445	0.3792082691160937	0.12992037421715608	0.1482066729138109
0.5614458450037321	0.32319500343480784	0.11543676326001442	0.21265904048506942
0.6363665691262939	0.2660247836050018	0.10130481511247609	0.30399399290119455
0.7198054734468116	0.20790226415636606	0.0876876171812794	0.43355629325257544
0.8129169082310087	0.14903550860694917	0.07474669189818135	0.6177628843571673
0.9170699472802668	0.08963524464890056	0.06263644690028392	0.8805726039488526
1.033897173471482	0.029914109797338766	0.05149755279322456	1.2572818945152056
1.1653569976191294	-0.029914109797338766	0.04144946858019295	1.800435561708559
1.3138139675134421	-0.08963524464890056	0.032582558170176246	2.5891630981063303
1.4821432470208165	-0.14903550860694917	0.02495051560492449	3.744155528864454
1.6738679412287918	-0.20790226415636606	0.018564108415709536	5.452097769788892
1.8933416121746534	-0.2660247836050018	0.013387488441818883	8.006263376861513
2.145993806251467	-0.32319500343480784	0.009338394879270824	11.875328334071545
2.4386647296695396	-0.3792082691160937	0.006293338088208658	17.822611142279463
2.7800680689846717	-0.4338640677187617	0.004097904475823055	27.117747215953976
3.1814412499350295	-0.48696674569809606	0.0025830926921683018	41.92262357320114
3.657475177082267	-0.5383262092858274	0.0015807827534237687	66.01620223603643
4.2276696497961455	-0.5877586049795791	0.0009415599134492133	106.20157190068788
4.9183526634276635	-0.6350869776952459	0.0005453042282610736	175.1405955662702
5.76576296728434	-0.6801419042271677	0.0003049997869381752	297.30896094699824
6.820887335531765	-0.7227620997499832	0.00016242082753832506	522.1176753124039
8.157294259937565	-0.7627949951937449	0.00008077588981359748	954.4527398959269
9.884289312564363	-0.8000972834304684	0.00003665063488089955	1830.417963708067
12.169963155779914	-0.8345354323267345	0.000014740319797992315	3719.7467675090556
15.28364511271759	-0.8659861628460676	5.054109250994349e-6	8117.066837845993
19.678953431941505	-0.8943368905344953	1.3947108874720773e-6	19366.157899552323
26.168717467688783	-0.9194861289164246	2.8316551169626493e-7	51822.50322060266
36.329306394116436	-0.9413438536413591	3.6357597278623005e-8	161516.57680062292
53.55560068801603	-0.9598318269330866	2.2296122675325307e-9	622216.7754332445
86.30923308485625	-0.9748838842217445	3.32223667644662e-11	3.2798803957197545e6
160.8732228413056	-0.9864461956515499	0.	2.880656250507084e7
396.4320475486722	-0.9944775909292161	0.	6.724307713324147e8
2091.8996773448594	-0.9989511111039503	0.	2.2330122223506357e11

TABLE IV. Density at the pseudospectral grid points and quadrature weights.